Mem. Fac. Eng., Osaka City Univ., Vol. 48, pp. 27–36 (2007)

A Numerical Study on Confinement Effect by Square Hoops in Reinforced Concrete Bridge Piers Osaka City University

Yasuhisa KITADA*, Hajime OHUCHI**, Hisao TSUNOKAKE*** and Tomoaki SATO****

(Received September 28, 2007)

Synopsis

This paper presents a numerical study on the confinement effect by square hoops in reinforced concrete (RC) bridge piers with a square cross section. A Parametric study was carried out on the mechanical behavior of the structure subjected to monotonic and cyclic horizontal actions with any load directions by means of three dimensional non-linear finite element analysis. As the result, noticeable results were obtained as follows: First, under the monotonic loading, confinement effect by square hoops was more effective the larger the angle of the applied load axis apart from the prescribed design principal axis. Second, under the cyclic loading, the maximum strength was around 20% higher than the corresponding design strength when the angle of the load axis was more than 15 degrees apart from the principal axis. Last, under the triangle loading, , the level of the peak strength for Y-component is smaller than the uni-axial loading result, and also, higher than the Y-component of the result with the cyclic loading for $\theta = 45^\circ$. And, the strain of lateral reinforcement greatly increases after the 4.0 % drift angle.

KEYWORDS: Reinforced Concrete Bridge Piers, Confinement Effect, Numerical Study, Bi-axial Bending

1. Introduction

A lot of researches on the dynamic loading capacity of RC bridge piers under uni-axial horizontal load have been already conducted. Furthermore, the confinement effect by lateral reinforcement such as hoop tie has been considered recently in Japanese earthquake resistant design codes [1),2)]. While, those under bi-axial load are required to established a rational seismic design method, because an actual ground motion in earthquake is essentially three-dimensional. A few researches of the RC columns under bi-axial horizontal load, however, have been conducted, i.e. by Chen et al.[3),4)] and Yoshimura et al.[5)]. Moreover, studies on the confinement effect by lateral reinforcement such as hoop ties under bi-axial loading can be hardly found.

In this paper, therefore, the RC column for bridge pier model under bi-axial horizontal load is examined numerically by using the three dimensional non-linear finite element analysis. The RC bridge pier model to be

* Sakai City, Japan
** Professor, Div. of Structural & Concrete Engineering
*** Research Associate, Div. of Structural & Concrete Engineering
**** JIP Techno Science Corp., Japan

analyzed herein is designed according to an existing design code[1]. The Loading axis has an inclined angle of 15, 30, or 45 degrees from a main standard bending axis. In addition, various loading cases, such as monotonic and cyclic ones are also considered. The result is discussed focusing both on the load - displacement relationships and the strain distribution in the plastic hinge zone of the pier.

2. MODEL

Figure 1 shows the front and cross-section views of the present bridge pier model. This column has a square cross section of 2.5 m in each side length, which is designed not to fail in shear but ductile flexural mode according with the code [1]. Design conditions are as follows: the normal stress equals to 1.0 MPa at the bottom of RC column, and natural period is 1.0 second, and it stands on the ground Type II which denotes diluvial and alluvial ground. The longitudinal reinforcement is, thus, decided as follows: the tensile reinforcement ratio is equal to 1.728 %, and volume ratio of dual square hoop ties is 0.469 % as shown in Fig. 2.

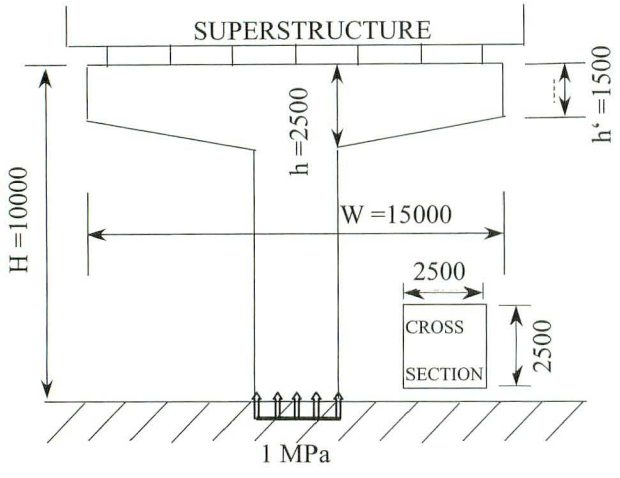

Fig. 1 Bridge Pier Model

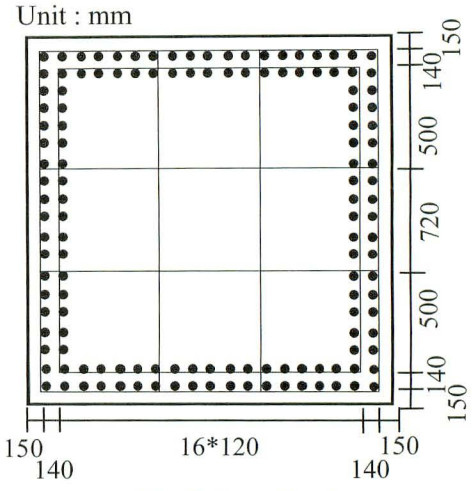

Fig. 2 Cross Section

3. NUMERICAL ANALYSES

3.1 Idealization of Bridge Pier Model

The three dimensional finite element analysis with material non-linearity was employed in the present study. Only the column member of the bridge pier model as shown in Fig. 1 was analyzed. Furthermore, material non-linearity was accounted exclusively on its bottom region, which is subjected to a predominant bending action to control the pier model failure. The height of the region was 1.2 times of the side length of the column cross section as shown in grayed area of Fig. 3. While, the longitudinal reinforcement arrangement of the model in Fig. 2 was put together to representative locations at the solid circles as shown in Fig. 4 with an equivalent total cross sectional area of the model. Moreover, solid, truss and beam elements were applied for concrete, longitudinal reinforcing bars and the hoop ties, respectively. The beam element, in particular, was necessary to reveal how the hoop ties work to generate the confinement effect. As the result, the column with reinforcement of the model was subdivided into 1923 elements with 1573 nodes.

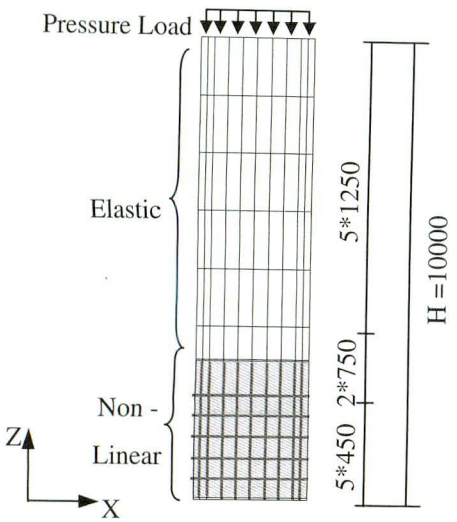

Fig. 3 Front View of Column Idealization

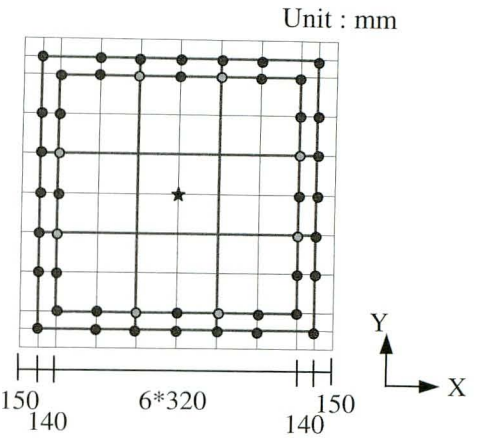

Fig. 4 Cross Section View of Idealization

3.2 Material Properties

Figure 5 shows the stress - strain relationship for the reinforcing bar that is bi-linear model and the strain hardening is also considered as 1.0 % of its elastic modules. While, as shown in Fig.5 (b), the Modified Ahmad Model is used for the stress-strain relationship for the concrete material. Yield conditions of the materials are von Mises and Ottesen's criterions [6], respectively. The concrete material factors: a to d in Tables 1 were suggested by Hatanaka et al. [7]. Moreover, the tensile softening is also introduced [8]. In addition, the material constants for concrete and reinforcement were shown in Table 2.

Table 1 Material Factor for Ottesen's Model

Fracture Model	Proposer	*a*	*b*	*c*	*d*
Ottesen	Hatanaka et al.[7]	1.2560	4.0300	14.6300	0.9870

Table 2 Material Constants for Concrete or Reinforcement

Concrete	Compressive Strength (f_c)	21.0 MPa
	Tensile Strength (f_t)	1.75 MPa
	Elastic Modulus (E_c)	23.5 GPa
	Poisson's ratio (ν_c)	0.167
Reinforcement	Yield Strength (f_y)	300.0 MPa
	Elastic Modulus (E_s)	200.0 GPa
	Poisson's ratio (ν_s)	0.3

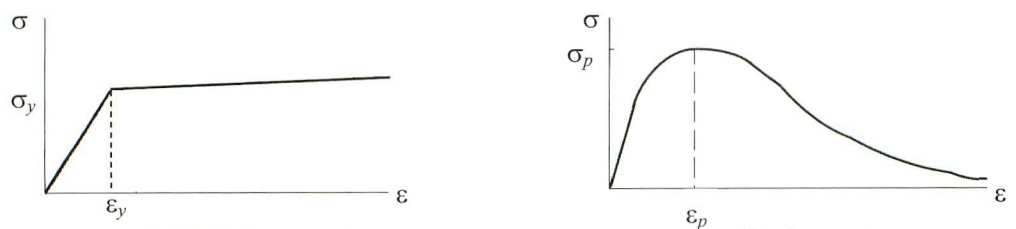

(a) Reinforcement (b) Concrete

Fig. 5 Stress-Strain Relationships

3.3 Various Loading Cases

In this study, the following three loading cases were examined as follows: First, the monotonic loadings for four directions were given as shown in Fig. 6(a). The loading directions are 15, 30, 45 degrees from the principal axis $\theta = 0°$ as a basic case. Second, the cyclic loading cases for the same directions as the monotonic ones were applied as shown in Fig. 6(b). Last, the triangle loading cases were adopted as the state of bi-axial bending is assumed as shown in Fig. 6(c).

In all cases, the displacement control loading was imposed. The applied displacements were set as magnifications of the drift angle. A unit drift angle was defined herein as horizontal displacement divided by the height from the bottom of the pier to the superstructure's centroid of its cross section, and the magnifications equal to 0.5 %, 1.0 %, 2.0 %, 3.0 %, 4.0 %, 5.0 %.

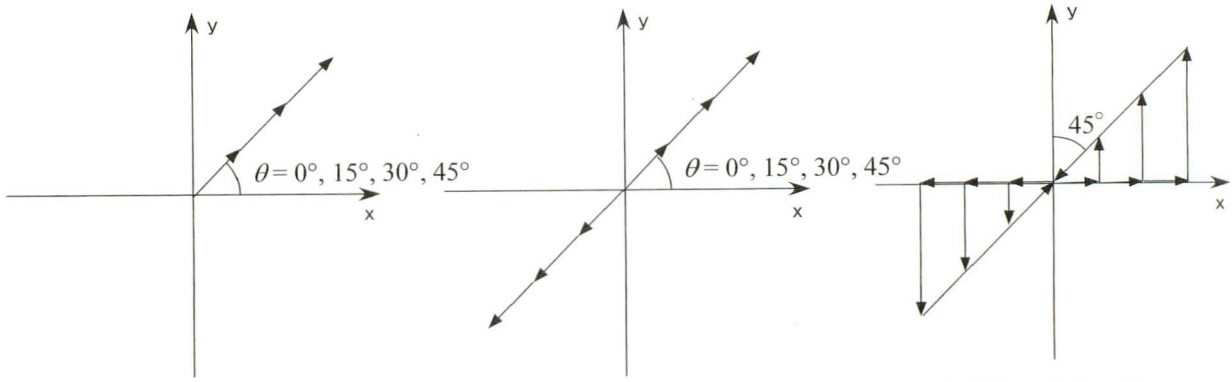

(a)Monotonic Loading (b) Cyclic Loading (c) Triangle Loading

Fig. 6 Loading Cases

3.3.1 Monotonic Loading Cases

Figure 7 shows the load (P) - displacement (δ) relationships for all loading cases, in which squares, circles and triangles indicate that the initial yielding, the maximum strength and the post peak strength at 10% reduction from the maximum value, respectively. From this figure, the maximum strength increased as the angle increased, and also that was around 30% higher than the corresponding design strength. No significant load reduction, furthermore, could be observed up to 5.0 % drift angle.

Next, the normal compressive stress distributions of concrete on the cross section at height of 0.36D (D: section depth) are as shown in Fig. 8 when the post peak strength decreased to 90% of the maximum strength. The shape of the distribution changed to be triangle as the angle for loading increased, though it was rectangle in the case of $\theta = 0°$. The high level stresses could be observed somewhat inside area from the corner in Fig. 8 (b) - (d), which was suggested the occurrence of compression failure in concrete. Because the stresses on and near the corner undergone the largest compressive strain were smaller than those of the above area, that stresses should be at compressive softening zone after the peak according to the stress - strain curve of Fig.5 (b).

Last, the strain distributions of hoop ties are shown in Fig. 9, as well as Fig.8. It can be confirmed that the strain distribution of the hoop agreed fairly with that of concrete in Fig. 8.

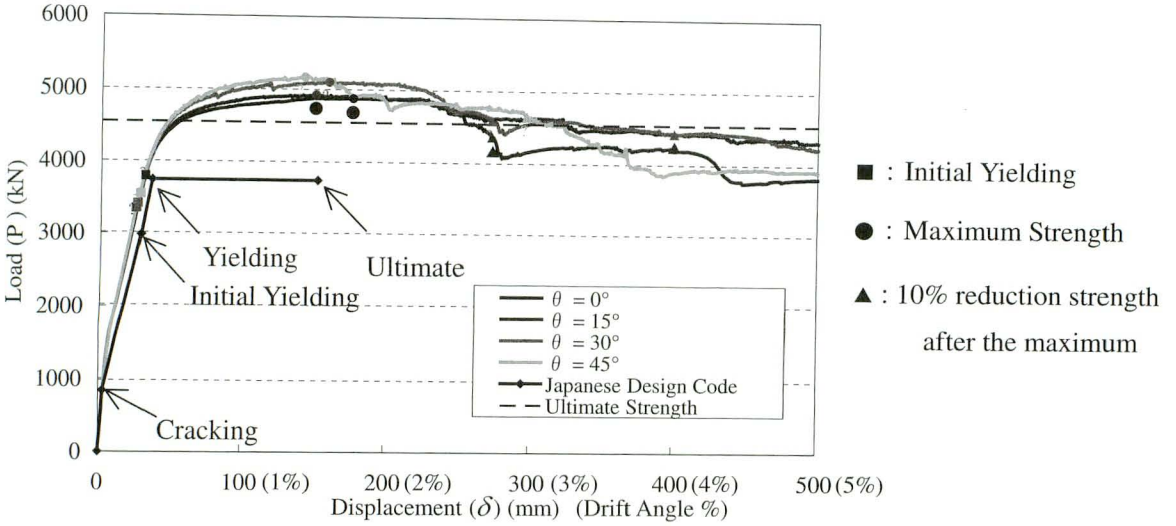

Fig. 7 Relationships of Load (P) – displacement (δ)

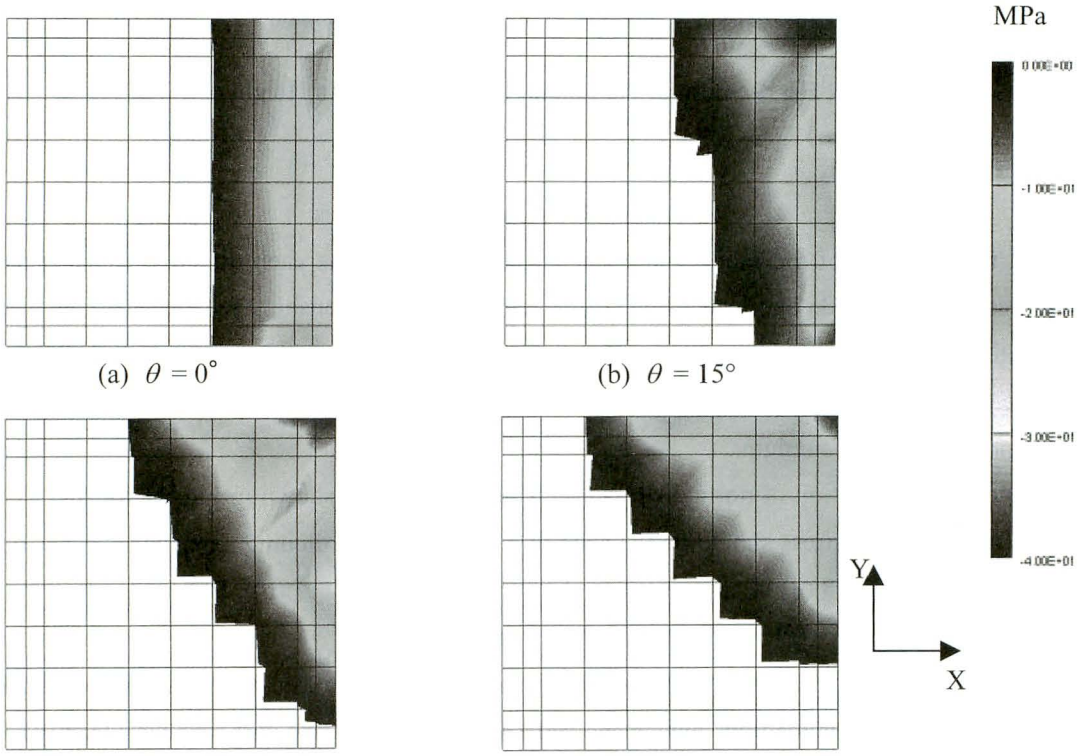

(a) $\theta = 0°$ (b) $\theta = 15°$

(c) $\theta = 30°$ (d) $\theta = 45°$

Fig. 8 Normal Stresses of the Cross Section in Height of 0.36D

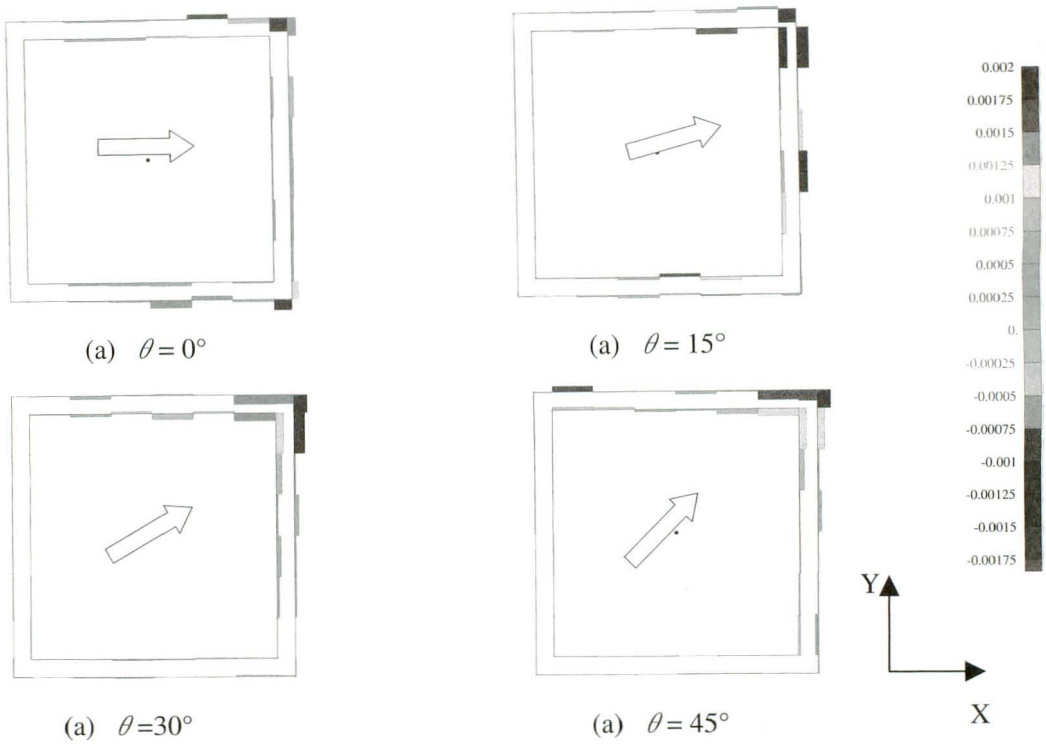

Fig. 9 Strain of the Lateral Reinforcement in Height of 0.36D

3.3.2 Cyclic Loading Cases

First, the behavior of the model under the cyclic loading to the each direction as same as the monotonic loading was also analyzed. The load (P) – displacement (δ) relationships for each loading cases are shown in Fig. 10 with the monotonic loading results. The displacement at the maximum strength increased compared with a monotonic load results for all loading cases. Furthermore, the maximum strengths were around 20% higher than the corresponding design strength.

Second, the distribution of normal stress at 3.0 % drift angle is shown in Fig. 11 for two loading cases ($\theta =$ 0°, 45°). The area those stress should be the state of a compressive softening expands than the case of monotonic loading as shown in Fig. 8 (d) in case of the loading for $\theta = 45°$(Fig. 11 (b)). But, it cloud not be little difference seen in loading for the $\theta = 0°$(Fig. 8 (a), and Fig. 11 (a)).

Third, the strain distributions of the hoop ties were also shown in Fig. 12. It differed obviously from those in Fig. 9 under the monotonic loadings, which showed a strain concentration with smaller intensity near the corner of the hoops. As to Fig.12 under the cyclic loadings, both no concentration and larger intensity beyond yielding could be observed.

Last, Fig. 13 shows the tensile strain at the corner of the hoop ties at each drift angles. Except for $\theta = 0°$, it can be confirmed generally that the strain of the hoops increased as the drift angle increased, although the numerical solutions were somewhat scattered because of the dual hoop ties arrangement of the pier.

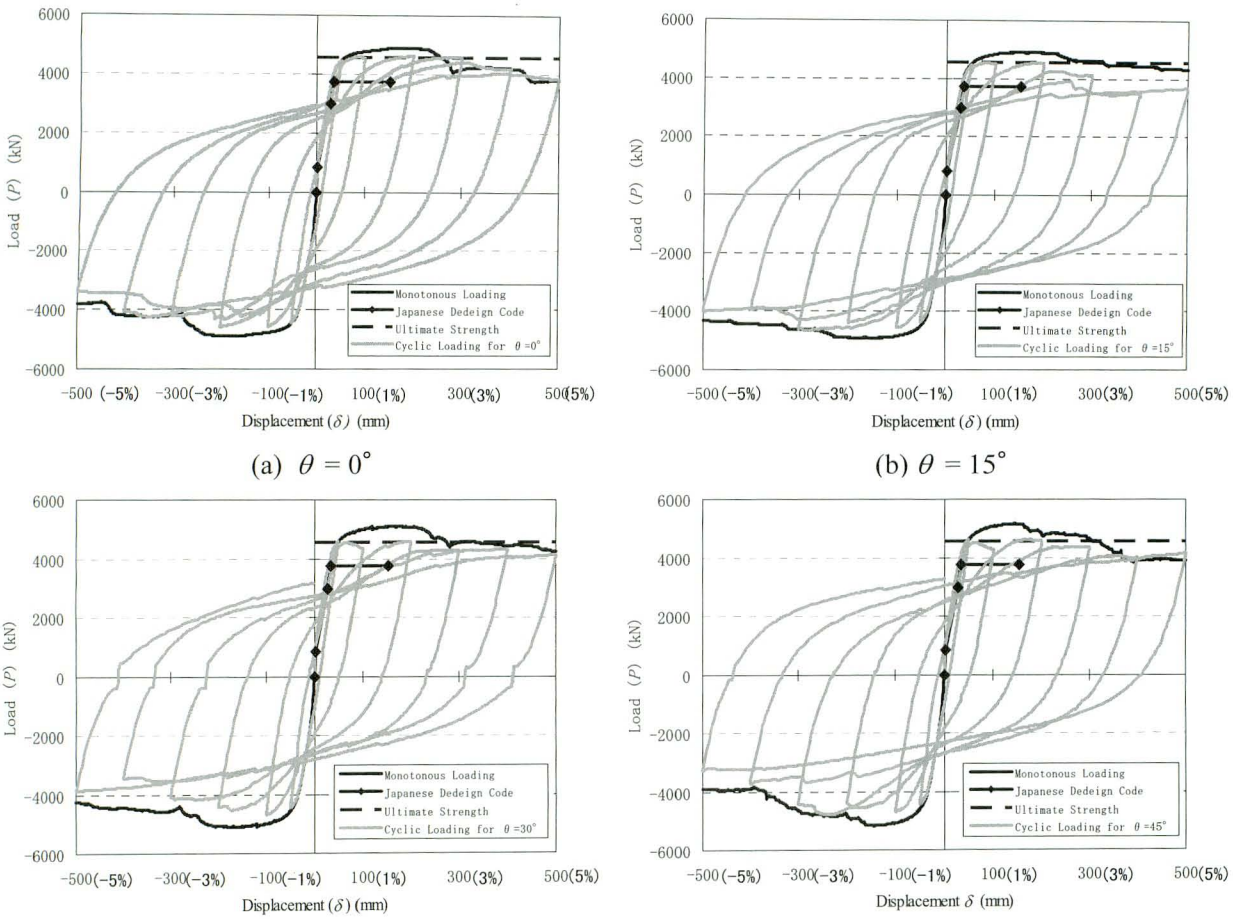

(a) $\theta = 0°$ (b) $\theta = 15°$

(c) $\theta = 30°$ (d) $\theta = 45°$

Fig. 10 Load (P) - Displacement (δ) Relationships (Drift angle %)

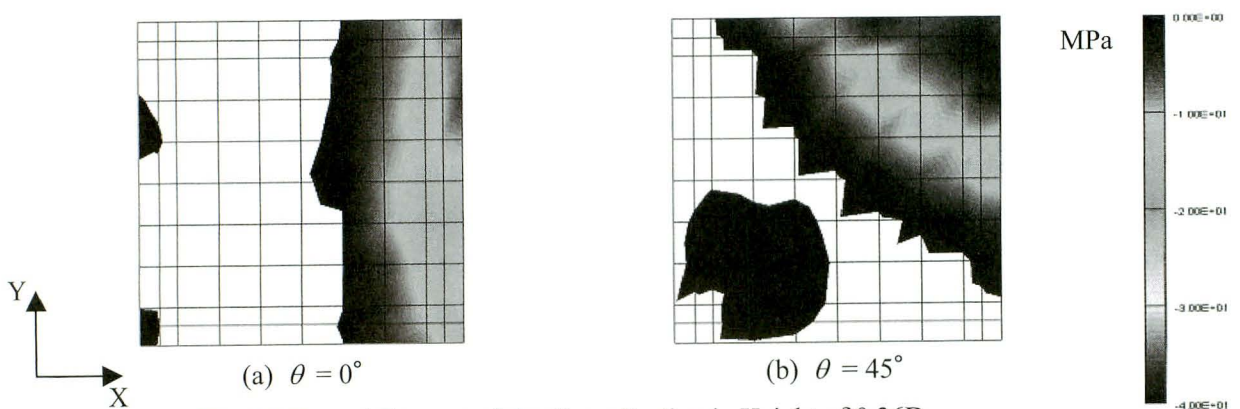

(a) $\theta = 0°$ (b) $\theta = 45°$

Fig. 11 Normal Stresses of the Cross Section in Height of 0.36D

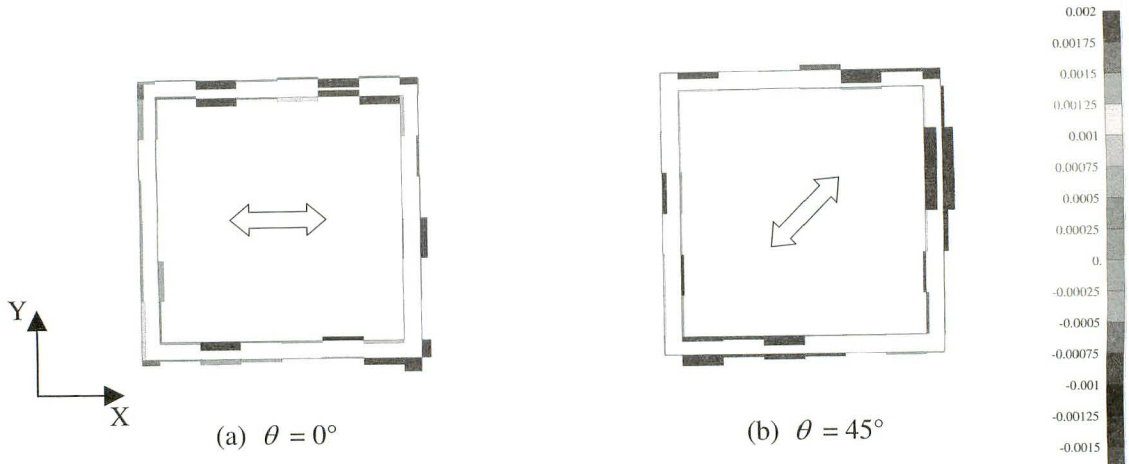

(a) $\theta = 0°$ (b) $\theta = 45°$

Fig. 12 Strain of the Lateral Reinforcement in Height of 0.36D

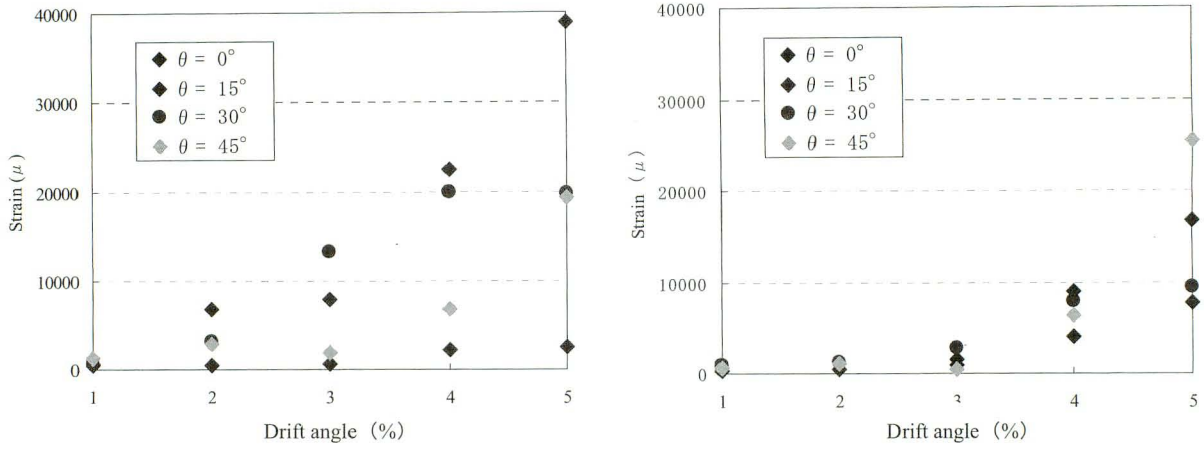

(a) Outer Hoop (b) Inner Hoop

Fig. 13 Variability of the Strain of Lateral Reinforcement

3.3.3 Triangle Loading Cases

Based upon the previous described results for the monotonic loading cases drawn that the strength decrease of the pier under the loading angle of 45 degrees could be observed the earliest loading stage, we examined here how the strengths and stress distributions of the pier depend on the loading direction angle.

Figure 14, therefore, shows the load (P) - displacement (δ) relationships under the triangular loadings as shown in Fig. 6(c). In this figure, the obtained gross horizontal force intensity and the displacement were decomposed into two components along the two crossing directions of X and Y as shown in Figs. 4 and 6. The maximum strength of X-component under the triangle loading indicated the red curve in Fig. 14 (a) was equal to that under cyclic loading for $\theta = 0°$of the black curve additionally drawn in Fig. 14(a). It could be said, thus, that there was a little influence of a combined loading of Y-direction on the maximum strength of X-direction.On the contrary, the maximum strength of Y-direction under the triangle loading as shown in Fig. 14 (b) was smaller than that under cyclic loading for $\theta = 0°$.

Furthermore, Fig. 15 shows the tensile strain at the corner of the hoop ties at each drift angles under the triangle

loading and also under the cyclic loading for $\theta = 45°$. As for the outside hoop ties, no dependency of the strain on the loading cases could be observed up to 3.0 % drift angle. Beyond 4 % drift angle, however, a distinct dependency could be recognized. Otherwise, no remarkable dependency for inner hoop ties was not confirmed.

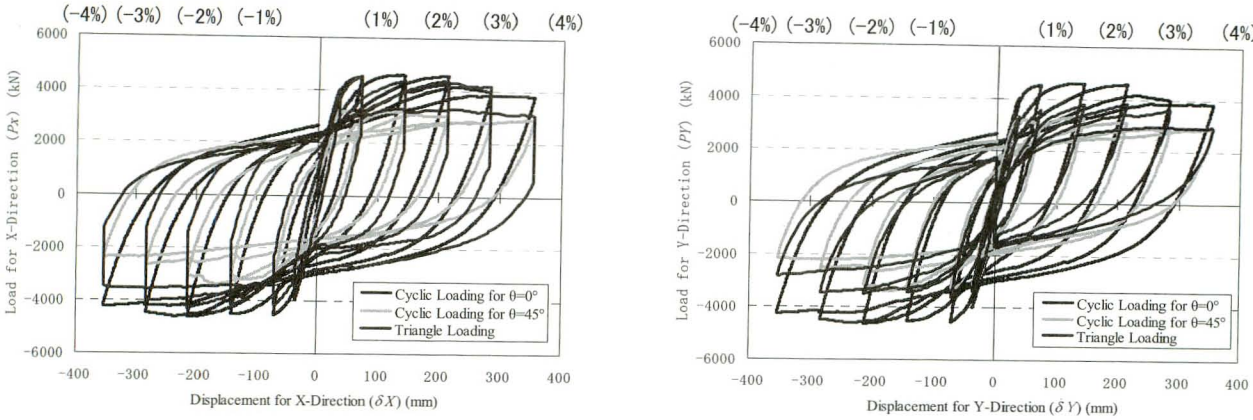

(a) X-Component (b) Y-Component

Fig. 14 Relationships of Load (P) - Displacement (δ) (Drift Angle %)

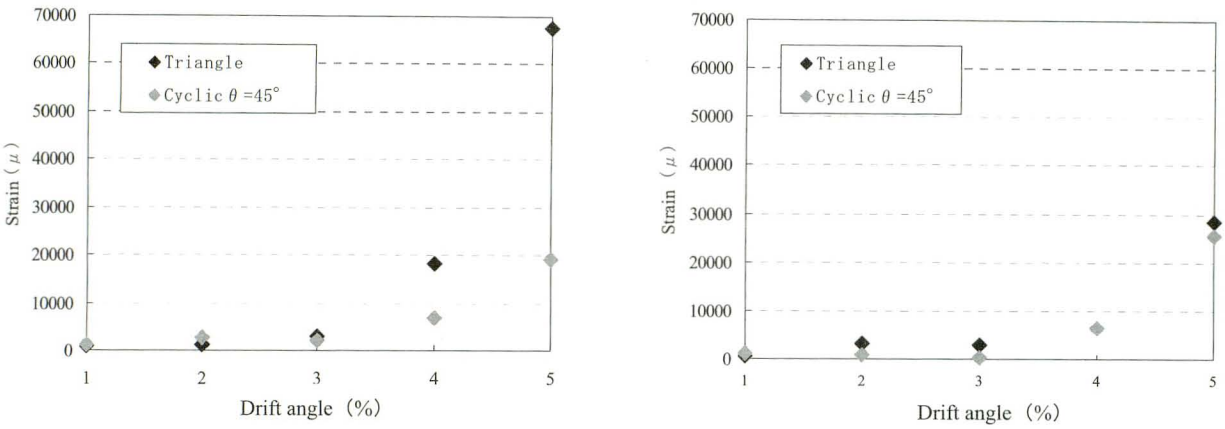

(a) Outer Hoop (b) Inner Hoop

Fig. 15 Variability of the Strain of Lateral Reinforcement

4. Concluding Remark

In this paper, numerical studies for the RC columns with a square cross section are carried out subjected to the three loading cases. As the result, the noticeable results were obtained as follows:

First, under the monotonic loading, the maximum strength increased as the angle increased, and also that was around 30% higher than the corresponding design strength. No significant load reduction, furthermore, could be observed up to 5.0 % drift angle. And, from the normal compressive stress distributions results, it was confirmed that the shape of the distribution changed to be triangle as the angle for loading increased, though it was rectangle in the case of $\theta = 0°$.

Second, under the cyclic loading, the displacement at maximum strength increased compared with the monotonic load results for all loading cases. Moreover, the maximum strengths were also around 20% higher

than the corresponding design strength. It could be also found that the tensile strains of the hoop ties increased more extensively than those under the monotonic loadings. And, it can be confirmed generally that the tensile strain of the hoops at the corner increased as the drift angle increased, although the numerical solutions were somewhat scattered because of the dual hoop ties arrangement of the pier.

Last, under the triangle loading as the bi-axial bending, it could be observed that there was a little influence of a combined loading of Y-direction on the maximum strength of X-direction. On the contrary, the maximum strength of Y-direction under the triangle loading was smaller than that under cyclic loading for $\theta = 0°$. And, from the tensile strain at the corner of the hoop ties at each drift angles, as for the outside hoop ties, no dependency of the strain on the loading cases could be observed up to 3.0 % drift angle. Beyond 4 % drift angle, however, a distinct dependency could be recognized.

Acknowledgement

The authors wish to thank Mr. Shimabata of Osaka City University for his help with the analyses.

5. References

1) Japan Road Association, Specifications for Highway Bridges: Part V- Seismic Design, Maruzen, Tokyo, 2002

2) Japan Society of Civil Engineers, Earthquake Resistant Design Codes in Japan, Maruzen, Tokyo, 2000

3) Chen, W. F. & Shoraka, M. T.: Tangent stiffness method for biaxial bending of reinforced concrete columns, IABSE Publications, 35(I), pp. 23-44, 1975

4) Chen, W. F. & Atsuta, T.: Theory of Beam-Columns, Vol. 2: Space behavior and design, McGraw-Hill, New York, pp. 253-260, 1977

5) Yoshimura M. et al.: Analysis of reinforced concrete structure subjected to two-dimensional forces, Journal of structural and construction engineering, Architectural Institute of Japan, No. 298, pp. 31-41, 1980

6) Chen, W. F.: Plasticity in Reinforced concrete, Trans. M. Shikibe, M. Kawakado, H. Adachi, Maruzen, Tokyo, pp. 207-252,1985.

7) K. Naganuma: Stress-strain relationship for concrete under triaxial compression, Journal of structural and construction engineering, Architectural Institute of Japan, No. 474, pp. 163-170, 1995

8) J. Izumo, H. Shima, H. Okamura: Analytical Model for RC Panel Elements Subjected to In-Plane Forces, Concrete Library International, JSCE, No. 12, pp. 155-181, 1989